Calculated cross sections for elastic scattering of slow positrons by silane

Alessandra Souza Barbosa and Márcio H. F. Bettega
Departamento de Física, Universidade Federal do Paraná, Caixa Postal 19044, 81531-990 Curitiba, Paraná, Brazil
(Received 6 June 2017; revised manuscript received 30 August 2017; published 26 October 2017)

In this work we investigate elastic collisions of low-energy positrons with silane (SiH_4). We employed the Schwinger multichannel method to calculate integral and differential cross sections for impact energies up to 10 eV. The calculations were performed within the static plus polarization approximation. We carried out a systematic study employing different schemes to account for the polarization effects of the target due the presence of the incoming positron. We investigate how the inclusion of extra functions in different extra (chargeless) centers affects the calculated cross sections and the physical phenomena such as the Ramsauer–Townsend minimum and the virtual state formation. Our results are compared with available experimental total cross sections and with integral and differential cross sections computed with a model correlation-polarization potential. In particular, our integral cross section agrees well with the experiment at low energies and our differential cross sections agree well with the results from previous calculations.

DOI: 10.1103/PhysRevA.96.042715

I. INTRODUCTION

There is an increasing interest in positron physics due to its fundamental, technological, and biological applications. In particular, the positron interaction with atoms or molecules is a cornerstone of this knowledge, since many of its applications is based on basic interactions of positrons with molecules and atoms [1–3]. Recent codes that simulate positron tracks in gaseous and liquid media use cross sections from positron collisions as input [4–6] in these simulations.

In a recent publication, Brunger and coworkers [7] presented a compilation of recommended cross sections for positron collisions with several molecules, including small diatomics, such as H_2, and large molecules, such as uracil. They tabulated the recommended cross sections for different types of processes, namely, elastic and inelastic scattering, vibrational excitation, positronium formation, and ionization and also tabulated recommended grand total cross sections. However, the authors found a lack of both theoretical and experimental results for several molecules.

Silane is one of the molecules that have received very little attention in positron scattering. This is a flammable (undergoes spontaneous combustion in air) and poisonous molecule, and therefore it is not easy to deal with this target experimentally. In fact, there are only two sets of experimental total cross sections measured by Mori *et al.* [8], published in 1985, and by Sueoka *et al.* [9], published in 1994. The data of Sueoka *et al.* [9] were corrected for the forward-angle scattering effect, which is an effect due to the limitation of the apparatus to discriminate the forward-scattered positrons.

From the theoretical side there are the calculations of Jain [10], Gianturco *et al.* [11], and Jain and Gianturco [12], where all calculations employ different approaches to the polarization and correlation potentials. The most recent theoretical study on low-energy (up to 10 eV) positron-silane collision was carried out by Jain and Gianturco [12] and was published in 1991. The authors reported integral, differential, and momentum transfer cross sections for energies up to 8 eV. They employed a new positron correlation-polarization potential, which provided results in better agreement with the experimental data of Mori *et al.* [8] than the previous calculations. Baluja and Jain [13] calculated total cross sections for positron scattering by silane for energies from 10 to 5 keV. The authors computed elastic and inelastic cross sections by using the spherical complex optical potential, including the static, correlation, and polarization potentials in the real part, and the absorption potential in the imaginary part. The authors reported that the calculated total (elastic plus inelastic) cross section agreed with experiment for energies above 50 eV.

In this work we report integral and differential cross sections for elastic scattering of positrons by SiH_4. The cross-section calculations employed the Schwinger multichannel method and were carried out within the static-plus-polarization approximation, for impact energies up to 10 eV. The positronium formation threshold value for SiH_4 reported by Refs. [10,11] is $E_{Ps} = 5$ eV. We estimated E_{Ps} by using the experimental ionization potential (IP) value of 11.2 eV [14] and the relation $E_{Ps} = IP - 6.8$ (in eV), and obtained $E_{Ps} = 4.4$ eV. Since our calculations do not take the real-positronium-formation channel into account, we do not expect agreement between our results and the experimental data above E_{Ps}. However, the description of the polarization effects of the molecular electronic cloud can, in principle, account for the virtual positronium formation. To investigate the influence of polarization effects on positron-silane scattering, we carried out a systematic study considering different schemes to account for polarization by expanding the space of configuration state functions and/or by including extra functions in extra (chargeless) centers. Some past works employing the Schwinger multichannel method have shown that the inclusion of extra functions or centers can be effective in the description of polarization effects for both electron and positron scattering [15–18]. Our integral cross sections are compared with experimental total cross sections and with theoretical results available in the literature. In particular, we observed a Ramsauer–Townsend minimum and a virtual state in our computed integral cross section. We discuss the different schemes to account for polarization effects with respect to these two physical phenomena and with the agreement between our results and the experimental data. We also compare our calculated integral cross section for silane with available experimental data and theoretical results for methane [19,20]. Despite the similarity of the molecular geometry of

both molecules, silane has a larger dipole polarizability than methane: $32.24a_0^3$ for silane and $16.52a_0^3$ for methane [21]. Due to the difference in the values of the polarizability of both molecules, we expect that the polarization effects play a larger role for silane than for methane. Differential cross sections are important for comparison with future calculations and experiments, and here our results are compared with the previous calculations of Jain and Gianturco [12]. These cross sections are also useful to experimentalists to correct the measured total cross sections for the forward-angle scattering effect [7].

The remainder of this paper is as follows: In Sec. II we present the theoretical method and the computational procedures employed in our calculations. In Sec. III we present and discuss our results in the light of a comparison with available experimental total cross sections and theoretical integral and differential cross sections. We also discuss the importance of polarization in the resulting cross sections. Section IV closes the paper with a brief summary of our results.

II. THEORY AND COMPUTATIONAL DETAILS

The elastic cross sections were computed with the Schwinger multichannel (SMC) method as implemented for positron-molecule collisions. This method has been described in detail in several publications [22,23], so here we only discuss those points that are relevant to the present calculations.

The working expression for the scattering amplitude is

$$f(\vec{k}_f,\vec{k}_i) = -\frac{1}{2\pi}\sum_{m,n}\langle S_{\vec{k}_f}|V|\chi_m\rangle(d^{-1})_{mn}\langle\chi_n|V|S_{\vec{k}_i}\rangle, \quad (1)$$

where

$$d_{mn} = \langle\chi_m|A^{(+)}|\chi_n\rangle \quad (2)$$

and

$$A^{(+)} = Q\hat{H}Q + PVP - VG_P^{(+)}V. \quad (3)$$

In the above equations, $|S_{\vec{k}_{i,f}}\rangle$ is a solution of the unperturbed Hamiltonian H_0 (the kinetic energy of the incoming positron plus the target Hamiltonian) and is a product of a target state and a plane wave, V is the interaction potential between the incident positron and the electrons and nuclei of the target, $|\chi_m\rangle$ is a set of $(N+1)$-particle configuration state functions (CSFs) used in the expansion of the trial scattering wave function, $\hat{H} = E - H$ is the collision energy minus the full Hamiltonian of the system ($H = H_0 + V$), P is a projection operator onto the open-channel space defined by the target eigenfunctions, and $G_P^{(+)}$ is the free-particle Green's function projected onto P space. Finally $Q = (\mathbb{1} - P)$ is the projector onto the closed electronic channels of the target.

In the static plus polarization (SP) approximation, the configuration space is composed by CSFs of the form

$$|\chi_{ij}\rangle = |\Phi_1\rangle \otimes |\varphi_j\rangle \oplus |\Phi_i\rangle \otimes |\varphi_j\rangle, \quad (4)$$

where $|\Phi_1\rangle$ represents the ground state of the molecule obtained at the Hartree–Fock (HF) level and $|\varphi_j\rangle$ is a single-particle orbital used to represent the positron scattering orbital (see below). $|\Phi_i\rangle$ is obtained from virtual single excitation of the target out of the HF reference state.

TABLE I. Relation between symmetries of C_{2v} and T_d groups.

C_{2v}	T_d
A_1	$A_1 + T_2 + E$
A_2	$A_2 + T_1 + E$
B_1	$T_1 + T_2$
B_2	$T_1 + T_2$

Although silane belongs to the T_d symmetry group, our calculations were performed in the C_{2v} group, since the SMC code deals only with Abelian groups. Table I shows the relation between the symmetries of both groups. Note that, if the same polarization criterion is employed; that is, the same number of holes, particles, and scattering orbitals are employed, the cross sections would not be affected by the symmetry group used in the calculations. In addition, most of the positron-molecule physics is discussed in view of the s-wave cross section, which belongs to the totally irreducible representation, regardless which symmetry group is employed in the calculations. All the calculations were carried out at the fixed Si–H internuclear distance of 1.48 Å [24] and employed the TZV++$(3d,3p)$ basis set, as implemented in the package GAMESS [25].

The polarization effects were taken into account through single excitations of the target from the hole (occupied) orbitals to a set of particle (unoccupied) orbitals. To study the description of the polarization effects in the calculated cross sections, we carried out several calculations employing different number of CSFs and extending the single-particle basis set. First we carried out two calculations employing the basis set mentioned above. A set of modified virtual orbitals (MVOs) [26] obtained through the diagonalization of a cationic Fock operator with charge +6 were used as particle and scattering orbitals. In the first calculation we employed the four valence occupied orbitals as hole orbitals, 67 MVOs as particle orbitals, and all nine occupied orbitals plus the first 67 MVOs as scattering orbitals ($4h67p76s$), resulting in 20 460 CSFs in this calculations. The second calculation employed 68 816 CSFs by using all nine occupied orbitals as hole orbitals, all 83 MVOs as particle orbitals and 92 scattering orbitals ($9h83p92s$). Then, we carried out six more calculations including one extra s-type function (exponent equal to 0.144), one extra p-type function (exponent equal to 0.2) and/or one extra d-type (exponent equal to 0.2) function at four, twelve, and twenty extra (chargeless) centers. The first four extra centers, together with the hydrogens, formed a cube centered at the Si atom. Then we included eight more extra (chargeless) centers, forming a bigger cube centered in the Si atom, with the half diagonal equal twice the Si–H bond. Finally, we carried out a calculation employing twenty extra (chargeless) centers, including the previous twelve and another eight placed in the vertex of a cube, also centered in the Si atom, with each center a distance from the Si atom equal to three times the Si–H bond. The details of the SP 1 to SP 7 calculations are summarized in Table II.

III. RESULTS

In Fig. 1 we show the present integral cross section (ICS) for the elastic scattering of slow positrons by silane computed

TABLE II. Number of hole (h), particle (p), and scattering orbitals (s), extra (chargeless) centers and additional Cartesian Gaussian functions labeled as (s,p) and (s,p,d), number of configuration state functions (CSFs) for each irreducible representation of the C_{2v} symmetry group, and total of CSFs employed for each calculation, labeled SP 1 to SP 7.

Label	Orbitals	Extra centers (functions)	A_1	B_1	B_2	A_2	Total
SP 1	$4h67p76s$	0	5677	5114	5114	4555	20460
SP 2	$9h83p92s$	0	19098	17200	17200	15318	68816
SP 3	$4h69p78s$	4 (s,p)	5883	5408	5408	4937	21636
SP 4	$4h69p78s$	4 (s,p,d)	5807	5414	5414	5023	21658
SP 5	$4h70p79s$	12 (s,p)	6001	5564	5564	5131	22260
SP 6	$4h69p78s$	12 (s,p,d)	5831	5431	5431	5035	21728
SP 7	$4h70p79s$	20 (s,p)	6099	5572	5572	5049	22292

within the static plus polarization (SP) approximation. These results were obtained employing the TZV++($3d,3p$) basis set in two different calculations; namely, $4h67p76s$ (SP 1) and $9h83p92s$ (SP 2). Despite the big difference in the number of CSFs employed in each calculation, the cross sections lie together in all energy ranges considered. We also compare both sets of calculated ICSs with the experimental total cross sections (TCSs) of Mori *et al.* [8] and Sueoka *et al.* [9], where the latter has been corrected for the forward-angle scattering. We also compare our results with the theoretical results of Jain and Gianturco [12], obtained with model correlation and polarization potentials. While our calculations are in very good agreement with the results of Jain and Gianturco, there is a considerable disagreement between the theoretical and the experimental results, indicating the necessity of further investigation in the description of polarization effects in the positron-silane scattering. We present below results obtained from several additional calculations, showing that the resulting cross sections are improved with respect to the results shown in Fig. 1.

Describing the positron-molecule interaction is more challenging than the electron-molecule scattering due to the difference in the sign of the static potential experienced by both projectiles. While the polarization potential for both projectiles is attractive, the static potential felt by the electron is attractive, whereas for the positron is repulsive. Since our calculations were obtained in the SP approximation, the overall potential felt by the incoming positron results from the combination between the repulsive and attractive potentials. If the description of polarization effects is not well balanced, it can cancel the net potential felt by the positron resulting in an unbalanced net potential and consequently in poorly described cross sections.

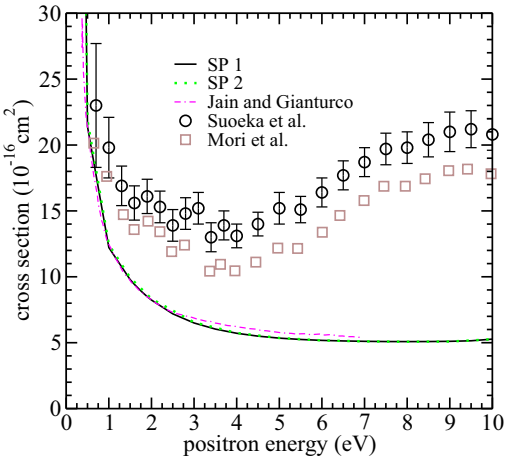

FIG. 1. Present positron-silane calculated integral cross section in the static-polarization approximation for energies up to 10 eV. We compare our calculated data with experimental TCSs of Mori *et al.* [8] and Sueoka *et al.* [9] and theoretical cross sections of Jain and Gianturco [12].

As mentioned above, to improve the description of the polarization effects in positron-silane scattering, we carried out additional calculations employing extra functions located in extra (chargeless) centers. Some previous results for both electron and positron scattering by molecules have shown that the inclusion of extra functions placed in extra (chargeless) centers can improve the description of the polarization effects [15–18]. Moreover, for positron collisions, the use of extra functions in chargeless centers facilitates the virtual positronium formation, since they bring the electronic cloud (attractive for the incoming positron) away from the nuclei (repulsive for the incoming positron). In the present work we carried out calculations employing 4, 12, and 20 extra centers, and the details of these calculations are summarized in Table II.

The results are presented and compared with the experimental results of Mori *et al.* and the calculated cross section of Jain and Gianturco [12] in Fig. 2, where the vertical arrow locates the positronium formation threshold E_{Ps} at the estimated value of 4.4 eV. The calculations labeled SP 3 and SP 4 employed four extra centers, which together with the hydrogen atoms of the molecule form a cube centered in the Si atom. The SP 3 calculation employed one extra s-type function and one extra p-type function centered on the extra centers, and the SP 4 also employed one d-type extra function on those centers. The inclusion of the extra functions in the four extra centers improves the description of the polarization effects, since it moves the calculated cross section towards the experimental data. Moreover, the mere inclusion of an extra d-type function improves even more the results presented here. To extend this investigation, we included eight more extra (chargeless) centers, placed in a cube centered in the Si atom and with half-diagonal equal two times the Si–H bond length, totaling twelve extra centers. We also carried out two calculations differing between them by the inclusion of an extra d-type function which were labeled as SP 5 and SP 6. Finally, we included eight more extra centers also placed in a cube with the Si atom, but with a half-diagonal equal three times the Si–H

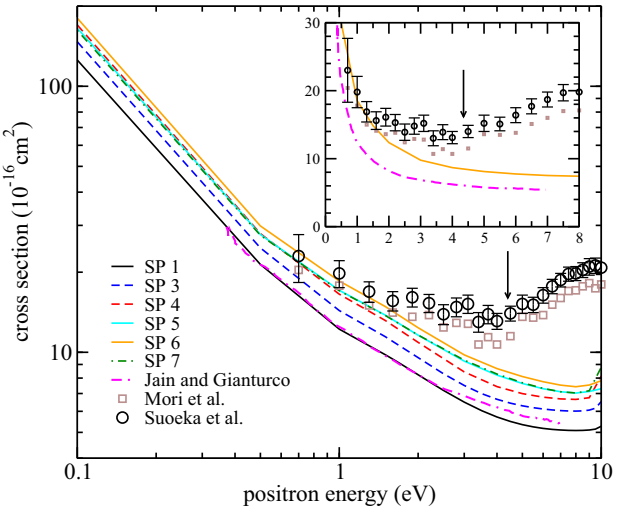

FIG. 2. Calculated positron-silane integral cross section employing different schemes, SP 1 up to SP 7, to account for the polarization effects (see text for details), for energies up to 10 eV. We compare our calculated results with experimental total cross sections of Sueoka *et al.* [9] and theoretical cross sections of Jain and Gianturco [12]. The inset compares our best ICS, calculated in the SP 6 approximation, with the available data from the literature on a linear-scale graph. The vertical arrow locates the estimated positronium-formation threshold E_{Ps} at 4.4 eV.

bond length. This calculation comprised 20 extra centers, is labeled SP 7, and employed only one extra *s*-type function and one extra *p*-type function.

As seen from Fig. 2, in general, the inclusion of extra functions increases the cross section at all energies. In particular, the SP 6 calculation, which includes one extra *s*-type function, one extra *p*-type function, and one extra *d*-type function in twelve extra (chargeless) centers, agree well with the experimental data at low energies (up to 2 eV) and corresponds to the best set of results among all schemes considered in our calculations. It is also noted from Fig. 2 that the calculated cross sections increase as the energy decreases (this point will be discussed later). Some of the calculations present some kinks at 10 eV, which may be related to pseudoresonances, which are associated with electronic channels that are above their excitation threshold but are treated as closed channels in the description of polarization. We also display in this figure an insert with the comparison of our best results with the available theoretical and experimental results from the literature on a linear-scale graph. Note that the experimental data increase above the positronium-formation threshold energy due to the contribution of the positronium-formation channel.

Silane can be seen as a methane analog, since both molecules present the same tetrahedral structure, and differs by the Si atom in silane replacing the C atom in methane. Despite this similarity, silane presents a larger polarizability ($32.24a_0^3$ and $16.52a_0^3$ for silane and methane [21], respectively) and a lower ionization energy (11.2 eV [14]) when compared with methane (12.6 eV [27]). In this sense, it is worth comparing the cross sections for both molecules. In Fig. 3 we compare our best ICS, calculated in the SP-6 approximation, with the Jain and Gianturco results [12], the experimental TCS [8,9], and the

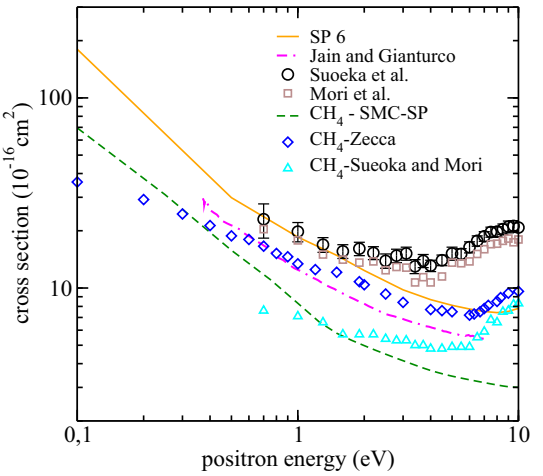

FIG. 3. Comparison of the present positron-silane calculated integral cross section, obtained in the SP 6 approximation, with available data of Zecca *et al.* [19] and Sueoka and Mori [20] for methane (CH_4). The experimental total cross sections of Sueoka *et al.* [9] and the calculated integral cross section of Jain and Gianturco [12], for silane, are also shown for comparison.

available results for methane: the experimental TCS and SMC calculations from Zecca *et al.* [19] and the experimental TCS from Sueoka and Mori [20]. From this figure it is seen that the cross sections for both molecules present the same trend, with silane cross sections in higher magnitudes than methane cross sections. It is also noted, that silane and methane experimental TCS present a minimum at around 4.5 and 6.0 eV, respectively, due the positronium formation cross sections which increase the TCS at energies higher than the positronium formation threshold. Since the present calculations do not include the positronium formation channel, it is not expected that our calculated ICS follows this trend.

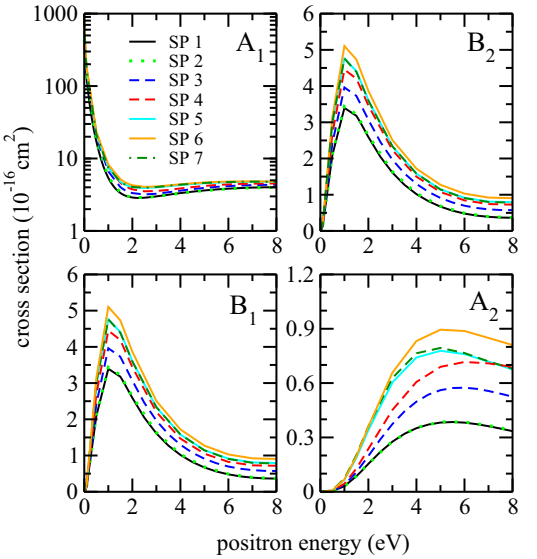

FIG. 4. Symmetry decomposition of the integral cross section according to the C_{2v} symmetry group.

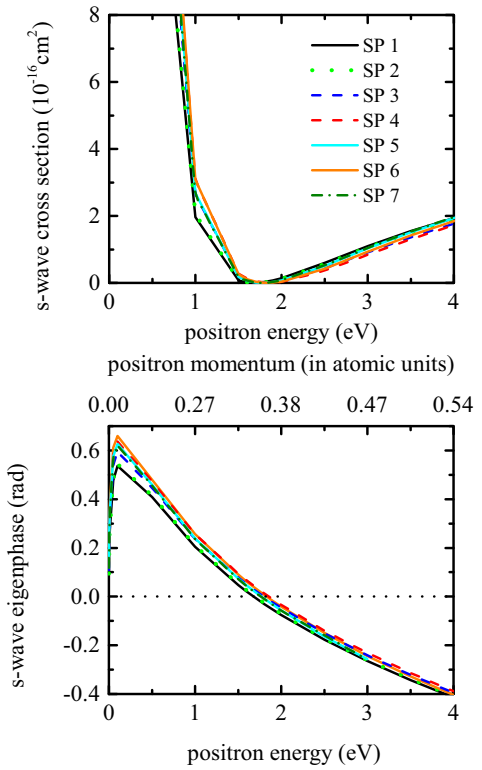

FIG. 5. Present positron-silane calculated s-wave cross section (top panel) and the corresponding s-wave eigenphase (bottom panel).

Figure 4 shows the symmetry decomposition of the ICS according to the C_{2v} group for all calculations from SP 1 to SP 7. Although silane belongs to the T_d symmetry group, the calculations being carried out in the C_{2v} do not affect the integral and the differential cross sections, which are usually compared with available experimental data and theoretical results. Only the symmetry decomposition of the integral cross section is affected. For example, as shown in Table I, the B_1 and B_2 symmetries of C_{2v} correspond to one component of each one of the three-fold-degenerate T_1 and T_2 symmetries of T_d. For this reason, the cross sections for the B_1 and B_2 symmetries are equal. The cross section of the totally symmetric irreducible representation A_1 shows a minimum at around 2 eV for all calculations and a large increase as the impact energy goes to zero. In positron-molecule collisions it is very common to observe the presence of a virtual state

TABLE III. Ramsauer–Townsend minimum (R-T min) position (in eV), and scattering length α (in units of a_0) for each calculation labeled SP 1 to SP 7.

Label	R-T min	α
SP 1	1.7	−10.9
SP 2	1.7	−11.2
SP 3	1.8	−12.9
SP 4	1.9	−14.6
SP 5	1.8	−14.3
SP 6	1.9	−15.7
SP 7	1.8	−14.0

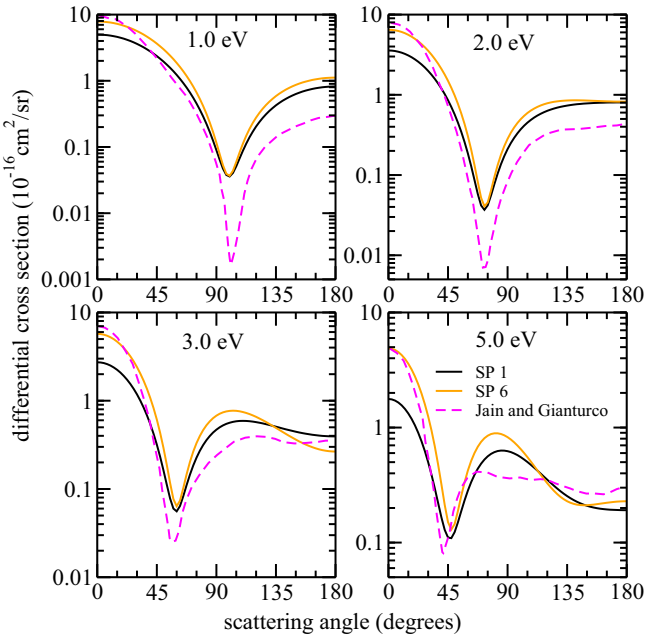

FIG. 6. Present positron-silane calculated differential cross section in the static plus polarization approximation compared with the results of Jain and Gianturco [12] at 1.0, 2.0, 3.0, and 5 eV.

and of a Ramsauer–Townsend minimum in the cross section. The virtual state is a resonance just above zero energy. It is related to large s-wave cross section at zero energy and to a negative value for the scattering length, and the s-wave eigenphase increases from zero towards $\pi/2$ at very low energies. In the ideal case, the cross section is $+\infty$ and the corresponding s-wave eigenphase is equal to $\pi/2$, both at zero energy, whereas the scattering length is equal to $-\infty$ [28]. The Ramsauer–Townsend minimum occurs due to the cancellation between the static and polarization potentials felt

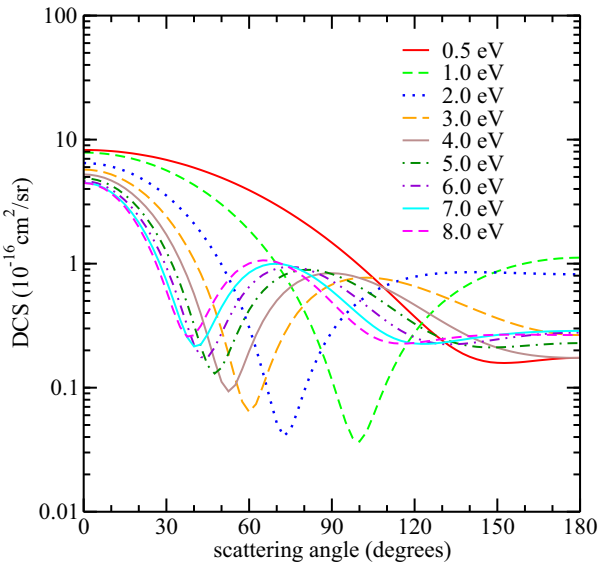

FIG. 7. Present recommended positron-silane elastic differential cross section calculated in the SP 6 approximation at energies ranging from 0.5 up to 8.0 eV.

TABLE IV. Recommended DCSs and ICSs for elastic scattering of positrons by silane, obtained in the SP 6 approximation. The tabulated data are in units of 10^{-16} cm^2.

Angle	Energy (eV)								
(deg)	0.50	1.00	2.00	3.00	4.00	5.00	6.00	7.00	8.00
0.00	8.25	7.87	6.47	5.73	5.24	4.88	4.62	4.48	4.47
10.0	8.09	7.59	6.07	5.24	4.68	4.26	3.96	3.76	3.68
20.0	7.61	6.80	4.99	3.96	3.29	2.79	2.41	2.14	1.97
30.0	6.86	5.65	3.54	2.40	1.71	1.25	0.94	0.73	0.60
40.0	5.94	4.32	2.11	1.08	0.570	0.321	0.222	0.215	0.264
50.0	4.93	3.00	0.983	0.293	0.112	0.145	0.275	0.446	0.627
60.0	3.91	1.86	0.307	0.0639	0.197	0.423	0.650	0.846	1.00
70.0	2.97	0.991	0.0520	0.202	0.503	0.751	0.912	0.998	1.03
80.0	2.14	0.416	0.0940	0.465	0.756	0.891	0.911	0.860	0.778
90.0	1.48	0.116	0.283	0.677	0.838	0.825	0.727	0.603	0.488
100	0.967	0.0367	0.498	0.767	0.767	0.649	0.506	0.386	0.303
110	0.606	0.112	0.673	0.746	0.620	0.465	0.342	0.266	0.233
120	0.374	0.278	0.784	0.657	0.465	0.328	0.254	0.227	0.229
130	0.240	0.483	0.839	0.546	0.341	0.250	0.225	0.231	0.246
140	0.177	0.688	0.854	0.443	0.258	0.217	0.229	0.249	0.261
150	0.159	0.867	0.848	0.363	0.210	0.211	0.245	0.266	0.267
160	0.162	1.00	0.836	0.307	0.186	0.218	0.262	0.278	0.267
170	0.170	1.09	0.825	0.276	0.176	0.226	0.274	0.285	0.266
180	0.174	1.12	0.821	0.266	0.174	0.228	0.278	0.287	0.266
ICS	29.6	18.5	12.4	9.78	8.68	8.11	7.75	7.53	7.42

by the incoming positron and affects the s partial wave at low energy [29]. In this case, the s-wave eigenphase crosses zero at the same energy where the s-wave cross section vanishes. To investigate these two effects, we computed the s-wave cross section and the respective s-wave eigenphase for each calculation, which are presented in Fig. 5. This figure shows the eigenphase versus the positron energy, in eV, on the lower axis, versus the positron momentum, in atomic units, on the upper axis. All of the s-wave cross sections vanish around 2 eV, in the same energy (around the positron momentum 0.38 a.u.) that their respective s-wave eigenphase crosses zero, changing from positive to negative, indicating that the net (static + polarization) potential changes from attractive to repulsive. This is the signature of the Ramsauer–Townsend minimum. Table III summarizes the minimum position for all calculations. With the s-wave eigenphase it is also possible to calculate the scattering length α, defined as [28]

$$\alpha = -\lim_{k\to 0}\frac{1}{k}\tan[\delta_0(k)], \tag{5}$$

where k is the positron momentum ($k = \sqrt{2E}$, where E is the impact energy) and δ_0 is the s-wave eigenphase. We employed the s-wave eigenphases obtained by the SMC method and used the approximation suggested by Morrison [30]. We obtained negative values for the scattering length, ranging from $-10.9a_0$ to $-15.7a_0$ (where a_0 is the Bohr radius), which are also summarized in Table III. These results indicate the presence of a virtual state for all calculations. In particular, the SP 6 scheme provides the most negative value for the scattering length of $-15.7a_0$, and the higher value for the position of the Ramsauer–Townsend minimum of 1.9 eV. These two results, along with the improvement of the present ICS in comparison with the results of Jain and Gianturco, and also with the good agreement of the SP 6 ICS with the experimental TCS at low energy, suggest that the polarization effects are better described by this scheme.

Figure 6 shows a comparison between our calculated differential cross sections (DCSs) obtained in the SP 1 and SP 6 schemes, where the latter is considered to be the best set of results, and the calculations of Jain and Gianturco [12] at 1, 2, 3, and 5 eV. In general, there is a good agreement in the angular behavior of the DCSs whereas their magnitudes present some disagreement. The agreement in the magnitudes of the calculated DCSs improves at 5 eV, where the polarization effects are less pronounced. Calculated elastic DCSs obtained in the SP 6 approximation are shown in Fig. 7 at energies ranging from 0.5 eV up to 8.0 eV and the tabulated data are presented in Table IV. When comparing the calculated DCSs for different impact energies, note that the angular behavior of the DCSs changes, with the well-defined minimum moving to lower angles as the impact energy is increased.

IV. SUMMARY

We presented integral and differential cross sections for elastic scattering of low-energy positrons by silane. We used different schemes for the inclusion of polarization effects, labeled SP 1 to SP 7. Chargeless extra centers were considered for inclusion of additional functions. The results were improved with the inclusion of extra functions, moving toward the experimental results. We also reported the presence of a Ramsauer–Townsend minimum at around 2 eV and of a virtual

state for all calculations, with scattering-length values vary from $-10.9a_0$ to $-15.7a_0$. We also calculated differential cross sections, which were compared with the results of Jain and Gianturco. Both calculations show the same shape, but differ in magnitude. In particular, the SP 6 calculation, which employed one extra s-type function, one extra p-type function, and one extra d-type function, centered in twelve extra (chargeless) centers, gives the best set of results, since that agrees better with the experimental data and describes better the virtual state and the Ramsauer–Townsend minimum. This suggests that not only is the number of extra (chargeless) centers important, but also the inclusion of an extra d-type function in those centers. In addition, it is important to note that the positions of the extra (chargeless) centers, employed in this work, was chosen in order to keep the molecular symmetry, whereas the choice of the exponents of the additional functions were rather arbitrary. However, as discussed by Lino *et al.* [15], there is a variational procedure to optimize the positions of the centers positions and exponents, which could be probably a further step in describing polarization effects in positron-silane molecules.

In a recent publication on recommended cross sections for scattering of positrons by molecules, the authors complained of the lack of results for some targets, silane being one of them. With this study we aimed at covering part of this lack of results for SiH_4 and also to stimulate other groups to do the same for this particular target and also for other molecules.

ACKNOWLEDGMENTS

A.S.B. acknowledges support from Brazilian Agency Coordenação de Aperfeiçoamento de Pessoal de Nível Superior (CAPES). M.H.F.B. acknowledges support from Brazilian agency Conselho Nacional de Desenvolvimento Científico e Tecnológico (CNPq), and from FINEP (under project CTInfra). The authors acknowledge computational support from Professor Carlos M. de Carvalho at LFTC-DFis-UFPR and at LCPAD-UFPR, and from CENAPAD-SP.

[1] C. M. Surko, G. F. Gribakin, and S. J. Buckman, J. Phys. B: At., Mol. Opt. Phys. **38**, R57 (2005).
[2] L. Chiari and A. Zecca, Eur. Phys. J. D **68**, 297 (2014).
[3] J. R. Danielson, D. H. E. Dubin, R. G. Greaves, and C. M. Surko, Rev. Mod. Phys. **87**, 247 (2015).
[4] C. Champion, C. Le Loirec, and B. Stosic, Int. J. Radiat. Biol. **88**, 54 (2012).
[5] M. J. Brunger, K. Ratnavelu, S. J. Buckman, D. B. Jones, A. Muñoz, F. Blanco, and G. García, Eur. Phys. J. D **70**, 46 (2016).
[6] F. Blanco, A. M. Roldán, K. Krupa, R. P. McEachran, R. D. White, S. Marjanović, Z. Lj. Petrović, M. J. Brunger, J. R. Machacek, S. J. Buckman, J. P. Sullivan, L. Chiari, P. Limão-Vieira, and G. García, J. Phys. B: At., Mol. Opt. Phys. **49**, 145001 (2016).
[7] M. J. Brunger, S. J. Buckman, and K. Ratnavelu, J. Phys. Chem. Ref. Data **46**, 023102 (2017).
[8] S. Mori, Y. Katayama, and O. Sueoka, At. Col. Res. Japan **11**, 19 (1985).
[9] O. Sueoka, S. Mori, and A. Hamada, J. Phys. B: At., Mol. Opt. Phys. **27**, 1453 (1994).
[10] A. Jain, J. Phys. B: At. Mol. Phys. **19**, L807 (1986).
[11] F. A. Gianturco, A. Jain, and L. C. Pantano, Phys. Rev. A **36**, 4637 (1987).
[12] A. Jain and F. A. Gianturco, J. Phys. B: At., Mol. Opt. Phys. **24**, 2387 (1991).
[13] K. L. Baluja and A. Jain, Phys. Rev. A **45**, 7838 (1992).
[14] S. K. Shin, R. R. Corderman, and J. L. Beauchamp, Int. J. Mass Spectrom. Ion Processes **101**, 257 (1990).
[15] J. L. S. Lino, J. S. E. Germano, E. P. da Silva, and M. A. P. Lima, Phys. Rev. A **58**, 3502 (1998).
[16] L. Chiari, A. Zecca, E. Trainotti, G. García, F. Blanco, M. H. F. Bettega, S. d'A. Sanchez, M. T. do N. Varella, M. A. P. Lima, and M. J. Brunger, Phys. Rev. A **88**, 022708 (2013).
[17] C. Winstead, V. McKoy, and M. H. F. Bettega, Phys. Rev. A **72**, 042721 (2005).
[18] A. S. Barbosa and M. H. F. Bettega, J. Chem. Phys. **146**, 154302 (2017).
[19] A. Zecca, L. Chiari, E. Trainotti, A. Sarkar, S. d'A. Sanchez, M. H. F. Bettega, M. T. do N. Varella, M. A. P. Lima, and M. J. Brunger, Phys. Rev. A **85**, 012707 (2012).
[20] O. Sueoka and S. Mori, J. Phys. B: At. Mol. Phys. **19**, 4035 (1986).
[21] T. N. Olney, N. M. Cann, G. Cooper, and C. E. Brion, Chem. Phys. **223**, 59 (1997).
[22] J. S. E. Germano and M. A. P. Lima, Phys. Rev. A **47**, 3976 (1993).
[23] E. P. da Silva, J. S. E. Germano, and M. A. P. Lima, Phys. Rev. A **49**, R1527 (1994).
[24] D. R. J. Boyd, J. Chem. Phys. **23**, 922 (1955).
[25] M. W. Schmidt, K. K. Baldridge, J. A. Boatz, S. T. Elbert, M. S. Gordon, J. H. Jensen, S. Koseki, N. Matsunaga, K. A. Nguyen, S. J. Su, T. L. Windus, M. Dupuis, and J. A. Montgomery, J. Comput. Chem. **14**, 1347 (1993).
[26] C. W. Bauschlicher, J. Chem. Phys. **72**, 880 (1980).
[27] NIST Chemistry Webbook (http://webbook.nist.gov/chemistry).
[28] C. J. Joachain, *Quantum Collision Theory* (North-Holland, Amsterdam, 1975).
[29] M. A. P. Lima, K. Watari, and V. McKoy, Phys. Rev. A **39**, 4312 (1989); B. M. Nestmann, K. Pfingst, and S. D. Peyerimhoff, J. Phys. B **27**, 2297 (1994).
[30] M. A. Morrison, Phys. Rev. A **25**, 1445 (1982).